Acta Geotechnica (2014) 9:399–412
DOI 10.1007/s11440-014-0312-5

RESEARCH PAPER

Thermo-mechanical behavior of energy piles in high plasticity clays

Ghassan Anis Akrouch · Marcelo Sánchez · Jean-Louis Briaud

Received: 23 September 2013 / Accepted: 27 February 2014 / Published online: 16 April 2014

Abstract Energy piles make use of constant and moderate ground temperature for efficient thermal control of buildings. However, this use introduces new engineering challenges because the changes of temperature in the foundation pile and ground induce additional deformations and forces in the foundation element and coupled thermo-hydro-mechanical phenomena in the soil. Several published full-scale tests investigated this aspect of energy piles and showed thermally induced deformation and forces in the foundation element. In parallel, significant progress has been made in the understanding of thermal properties of soils and on the effect of cyclic thermal load on ground and foundation behavior. However, the effect of temperature on the creep rate of energy piles has received practically no attention in the past. This paper reports the experimental results of an in situ tension thermo-mechanical test on an energy pile performed in a very stiff high plasticity clay. During the in situ test, the pile was subjected to thermal loading by circulating hot water in fitted pipes, simulating a thermal load in a cooling-dominated climate, at different levels of mechanical loading. The axial strain and temperature in the pile, and the load–displacement of the pile were monitored during the tension test at different locations along the center of the pile and at the pile head, respectively. The data showed that as the temperature increases, the observed creep rate of the energy pile in this high plasticity clay also increases, which will lead to additional time-dependent displacement of the foundation over the life time of the structure. It was also found that the use of geothermal piles causes practically insignificant thermally induced deformation and loads in the pile itself.

Keywords Creep · Energy piles · In situ tests · Strains · Stresses · Temperature effect

G. A. Akrouch (✉) · M. Sánchez · J.-L. Briaud
Zachry Department of Civil Engineering, Texas A&M University, College Station, TX 77843-3136, USA
e-mail: ghassan.akrouch@gmail.com

M. Sánchez
e-mail: msanchez@civil.tamu.edu

J.-L. Briaud
e-mail: briaud@tamu.edu

1 Introduction

Air pollution is one of the main environmental problems mankind faces in the twenty-first century due to the extensive use of fossil fuels. One of the opportunities to overcome this problem is to develop new technologies and methods to profit from the energy stored in the ground. A promising high-efficiency technology is the shallow geothermal energy system (SGES) [19, 22]. The use of SGES is growing rapidly because it consumes less conventional energy for operation, which in turn results in fewer CO_2 emissions [4, 22]. This technology harnesses constant and moderate ground temperature for thermal control of a building. Outside air temperature changes with the season, while ground temperature remains relatively constant. In summer, ground temperature is lower than air temperature, and so the ground may be used as a heat sink. The opposite is true in winter; the ground becomes a heat source. The system works by circulating a heat-carrying fluid through fitted high-density polyethylene pipes in the piles. The heat-carrying fluid is circulated at low temperatures when building heating is needed and at high temperature when cooling is required.

Because the engineering properties of the pile and soil materials are temperature dependent [17, 20, 33], this thermal loading results in volumetric expansion and contraction in the pile and complex coupled thermo-hydro-mechanical phenomena in the soil.

The knowledge on the thermo-mechanical behavior of energy piles is progressively growing thanks to the increasing number of thermo-mechanical full-scale load tests that have being performed and reported in the literature. All the reported tests [2, 5, 6, 13, 24, 26–28, 31, 34] concluded that the use of energy piles as ground heat exchangers for SGES induces an increase or decrease in stress and strain (when operating in cooling or heating mode, respectively) and load redistributions in the pile. From the information gathered in those tests, it was possible to relate the change in the mechanical response of the tested piles to the increased temperature level, soil strength, and boundary conditions.

All the thermo-mechanical tests on energy piles reported in the literature correspond to load (compression) tests. In those tests, both vertical side shear and point-tip pile resistance are engaged during loading. In this paper, the interest focuses on the impact of temperature on shear resistance only; for this reason, tension (pull-out) tests (i.e., no effect of point-tip pile resistance) have been performed. The thermo-mechanical tension tests were performed in the field on an energy pile installed in very stiff high plasticity (CH) clays. The tested pile was installed and instrumented at the National Geotechnical Experimentation Site (NGES) at the Riverside campus of Texas A&M University. A tension load test was performed on the pile, and it was subjected to thermal cyclic loading for 5 days under different mechanical load levels. Additional information gathered during the test included the temperature and relative humidity of the air, and the temperature of the water circulating in the pile.

One of the aims of this test was to investigate the time-dependent performance of energy piles in high plasticity clayey soils where soil creep might be an important factor to consider. In addition, this paper evaluates the load redistribution in the energy pile subjected to a thermo-mechanical load.

2 Conceptual background

The thermo-mechanical behavior of energy piles was described by Bourne-Webb et al. [13] and Amatya et al. [2] using a simple approach based on a review of thermo-mechanical load tests on energy piles. When analyzing an energy pile, the load distribution and strain profile are both of great importance. Under mechanical load only, the stresses in the pile are directly related to strains. When the vertical pile is subjected to thermal load, it experiences additional thermal strains, referred as ε_{T-Obs} which is the measured strain resulting from the thermal load, around a neutral point (NP). The NP is defined as the point where there is no change in strain due to the thermal load in the pile. When the pile is heated, it experiences expansion and it moves upward above the NP and downward below it, while the opposite is correct when the pile is cooled, it experiences contraction and it moves downward above the NP and upward below the NP. Another part of the vertical strain is restrained due to soil resistance ($\varepsilon_{T-restrained}$). The sum of $\varepsilon_{T-observed}$ and ε_{T-Rest} is the free strain (ε_{T-free}), which is the strain that the pile would experience if it was not inhibited by the soil and the structure. The thermal stresses (σ_T) resulting from the difference between the free and observed strain and the thermally induced load, P_T, can be calculated using Eq. 1. In this equation, the negative sign means that the restrained thermal strains result in a force in the opposite direction of the pile movement.

$$\begin{aligned} P_T &= -EA\varepsilon_{T-restrained} = -EA(\varepsilon_{free} - \varepsilon_{T-observed}) \\ &= -EA(\alpha\Delta T - \varepsilon_{T-observed}) = \sigma_T A \end{aligned} \quad (1)$$

where α is the linear coefficient of thermal expansion, E is the Young's modulus of the pile material, and A is the cross-sectional area of the pile. In energy piles, the total load in the pile is the sum of the mechanical and thermal load. More details about this approach are presented in Bourne-Webb et al. [13] and Amatya et al. [2].

Understanding the long-term behavior of energy piles and in particular their displacements is very important to limit their impact on the structural integrity of the building. This may be accomplished by limiting the additional deformation to within-tolerable limits. During their lifetime, piles exhibit creep, related to the time-dependent movements under a constant mechanical load applied by the superstructure. The creep rate is dependent on soil type, soil texture, applied stress level, and temperature. This last factor is more significant in clayey soils [10, 15, 29, 30]. As an example, Fig. 1 presents the experimental results of a triaxial creep test performed by Mitchell et al. [30] on undisturbed San Francisco Bay mud samples. The strain rate and strain increased after raising the soil sample temperature by 16.7 °C, which is close to the typical temperature increase in geothermal applications. The strain rate of the samples increased by a factor of approximately 10, after the start of the temperature change. In addition, Fig. 1b shows that the strain rate decreased with an increase in strain, but more slowly for higher temperatures.

There are some additional experimental studies looking at the effect of temperature on the time-dependent response of clays; they are mainly focused on the behavior of the Boom clay, a material studied in the context of the design of nuclear waste disposal (e.g., [14, 16, 18, 35, 37]).

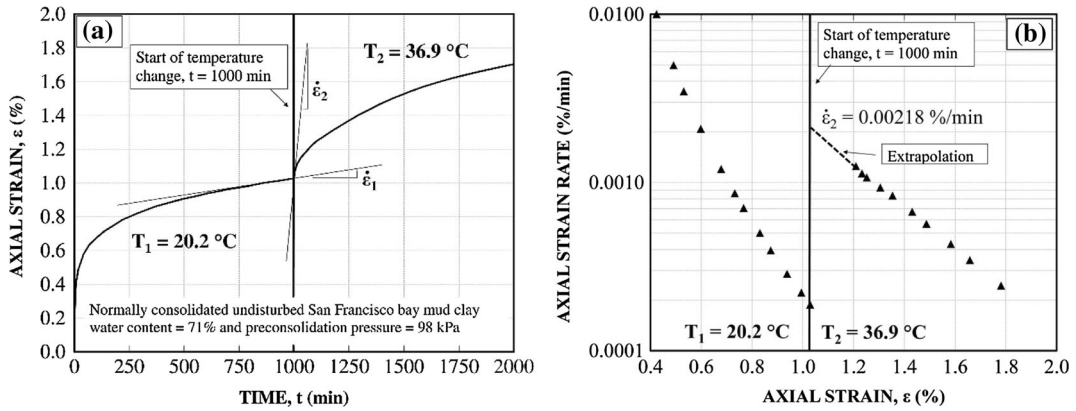

Fig. 1 Axial strain versus time **a** and strain rate versus axial strain **b** of an undisturbed San Francisco Bay mud sample subjected to temperature change (modified from Mitchell et al. [30])

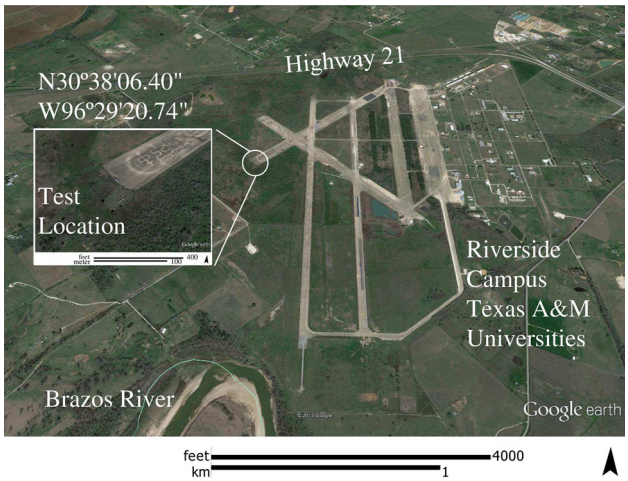

Fig. 2 NGES clay site location from Google Earth

Romero et al. [35] found that the effect of temperature on normally consolidated samples of Boom clay is quite noticeable, while the impact of temperature on creep rate for over-consolidated samples is practically negligible.

Based on extensive in situ creep tests on grouted anchors at the National Geotechnical Experimental Site (Texas A&M University), Briaud [9] proposed the following model (2) to evaluate the time-dependent displacement of anchors and piles:

$$\frac{S_t}{S_1} = \left(\frac{t}{t_1}\right)^n \tag{2}$$

where n is the viscous exponent; t (min), t_1, S_t (m), and S_1 (m) are the time, reference time, the displacement at time t, and the displacement at time t_1, respectively. The viscous exponent can be evaluated from field creep test or from the pressuremeter test [10]. The value of n is obtained as the slope of the plot of log S_t/S_{t1} versus log t/t_1 from field creep test and as the slope of the plot of log E_t/E_{t1} versus log t/t_1 from pressuremeter test [10, 11]. E_t and E_{t1} are the secant modulus measured during a pressure holding step from a pressuremeter test corresponding to t and t_1, respectively.

3 Test location materials properties

The in situ test was performed at the NGES at Texas A&M University, Riverside campus, which is located 12 km west of the main University campus (Fig. 2). Two main sites are located at the NGES: clay and sand sites. The soil properties of the two sites were reported in previous studies [7, 12, 21, 23, 32, 36, 38]. The experiment reported in this paper was conducted on a pile installed at the clay site.

The clay site covers an area of approximately 5,500 m^2. Briaud [8] summarized many of the laboratory and in situ tests performed at the site since 1980, and concluded that the stratigraphy of this site is composed of four layers. The top layer is red and gray very stiff high plasticity clay of a uniform thickness (about 5.5 m). The second layer is a sand layer with variable thickness averaging 1 m. Below this layer is dark gray clay-shale with interbedded fine-grained sand layers with an average thickness of 6.5 m. The fourth layer is a very hard dark clay (shale) layer that extends to a depth of 50 m. The soil stratigraphy, laboratory tests results, in situ tests results, and average soil properties of each layer are summarized in Fig. 3.

The compressive strength of the grout used for the tested pile was measured in the laboratory by unconfined compression on 0.05 m diameter samples. The measured compressive strength at 28 days ranged from 22.5 to 27.6 MPa, with an average of 25.7 MPa. The unit weight of the grout was 18.4 (kN/m^3), and the elasticity modulus was estimated from the compressive strength to be 17,400 MPa. The PEX pipes used to circulate the water in

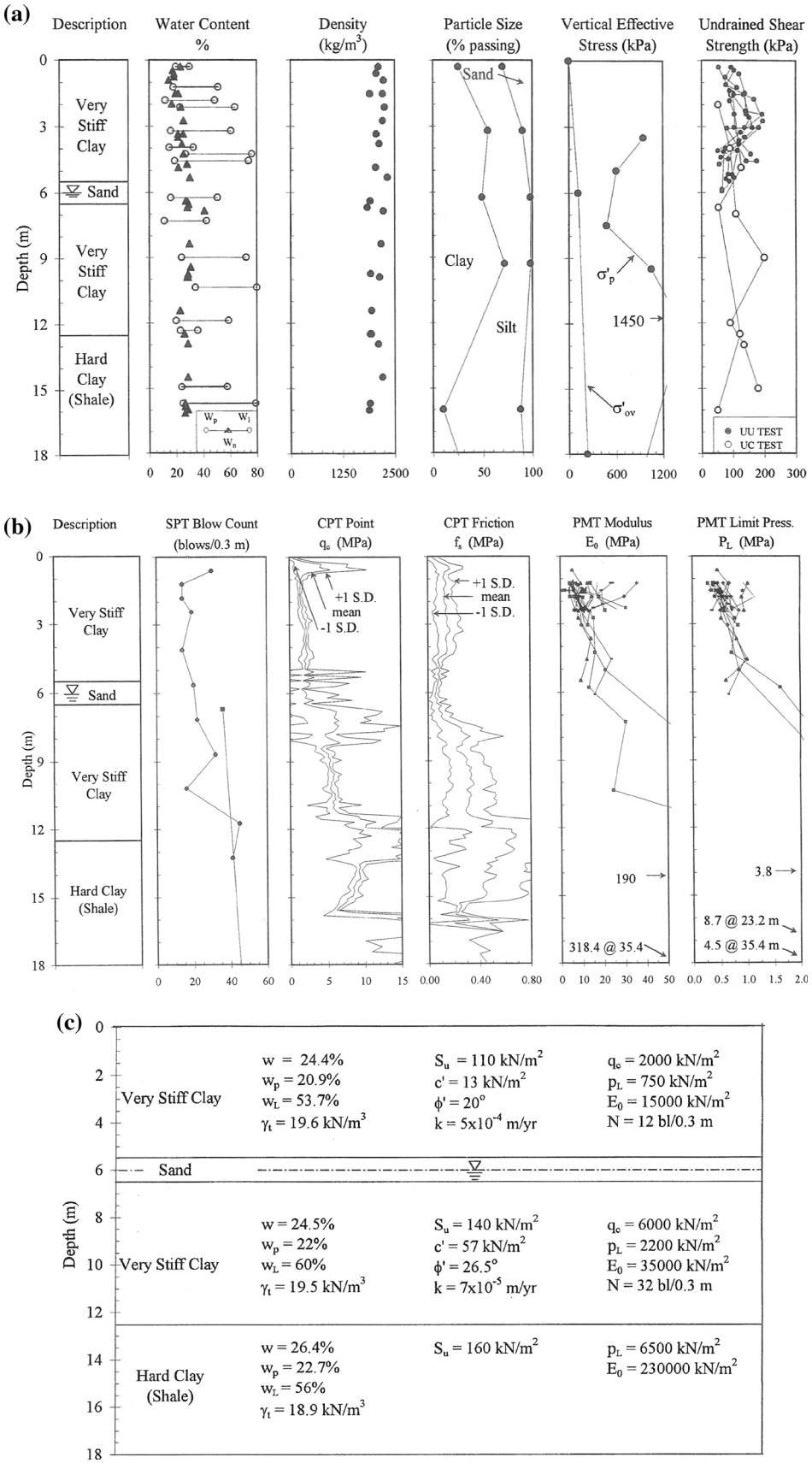

Fig. 3 Summary of soil properties and stratigraphy from laboratory tests **a**, field tests **b**, soil profile **c** at NGES-TAMU clay site (From Briaud [8])

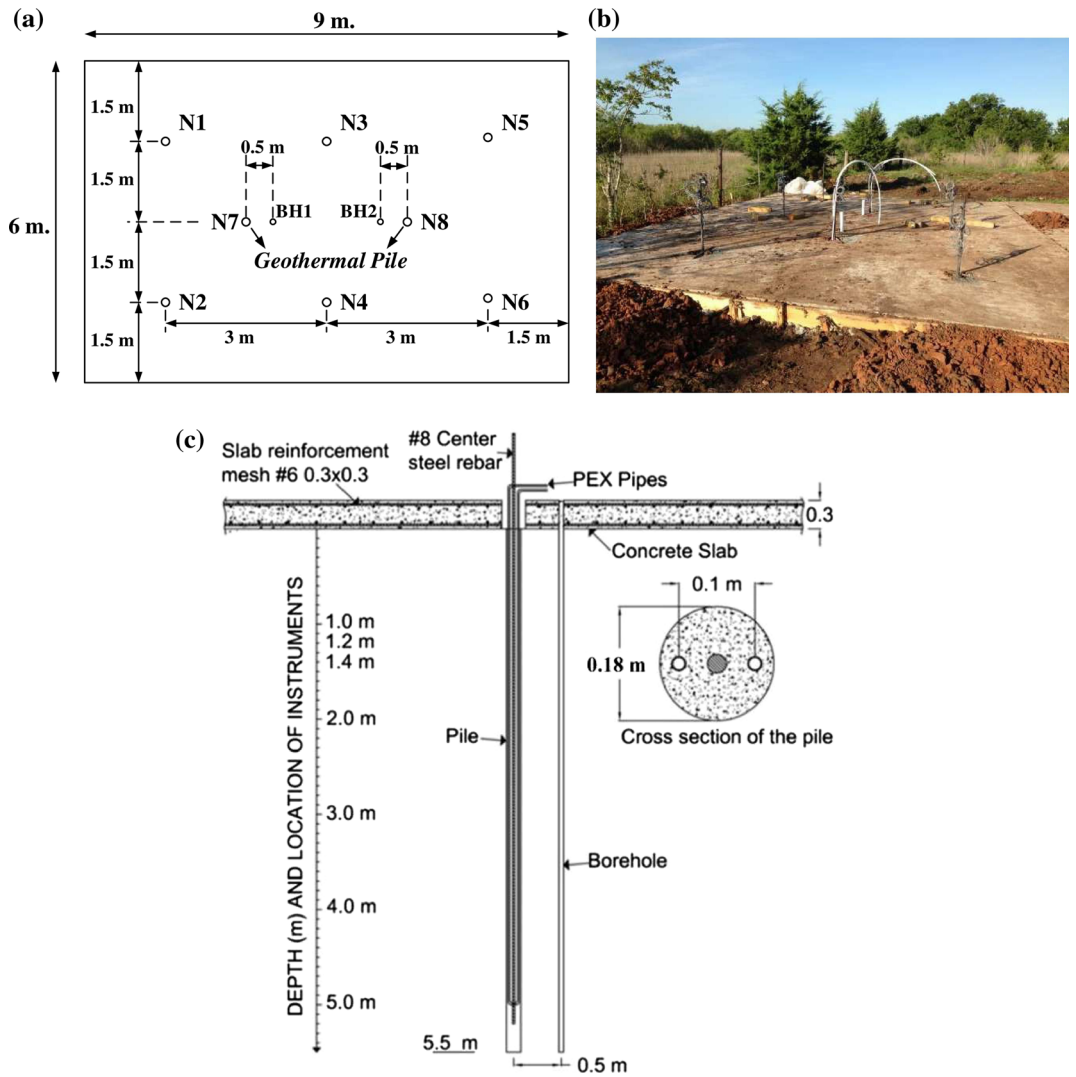

Fig. 4 **a** Pile layout with slab dimensions; **b** picture of mat; **c** cross section and plan view of the pile

the piles conform to ASTM F876/F877 standards as per the manufacturer.

4 Test layout and setup details

The tension test layout and details are shown in Fig. 4. The tested pile was one of the groups of eight piles installed at the NGES clay site labeled N1 to N8. Two of the eight piles were energy piles; the remaining six were used to study the creep of piles under mechanical loading only. The piles were drilled on July 17, 2013, and were grouted up to the ground level on the same day. The instrumented steel rebar and pipes were inserted in the drilled holes immediately after finishing the drilling process and before grouting. All the piles were 0.18 m in diameter and 5.5 m long. The hole in the slab is 30 cm in diameter, so slab and the pile are not connected. Each of the piles was reinforced with a 25-mm-diameter steel bar placed at the center of the drilled hole; the steel was of grade 75 with a yield stress f_y equal to 517 MPa and an elasticity modulus E_{Steel} equal to 204,000 MPa. The two energy piles were each fitted with 19-mm inner diameter and 23-mm outer diameter PEX pipes U-shaped loops. The pipe legs of the U were 0.1 m apart center to center and were bent at a distance of 0.4 m from the bottom of the pile. A concrete slab ($9 \times 6 \times 0.3$ m^3) was used as a platform to drill the piles and to perform the load test. The slab was reinforced with #6 bars in a mesh of 0.3 m $\times$ 0.3 m. When the slab was poured, eight circular openings of 0.3 m diameter and two circular opening of 0.15 m diameter were kept in the slab at the location of the eight nails and the two boreholes, respectively. This ensured an easy drilling and pile installation process. The boreholes are located at 0.5 m c/c from

Table 1 Instrumentation summary

	Instrument	Measurement	Number used
Mechanical measurement	Strain gauge model UFCA-5-11 installed along the pile at depth $z = 1$, 1.2, 1.4, 2.4, 3.4, and 4.4 m	Strain in the pile	6
	Dial gauge	Pile head displacement	2
	Pressure gauge	Pressure applied on the loading frame	2
	Load cell model 3000 from Geokon	Load applied on the pile	1
Thermal measurements	Thermocouple type T from Omega, installed along the pile and borehole	Temperature along the pile and the borehole adjacent to the pile	12
	at depth $z = 1$, 1.2, 1.4, 2.4, 3.4, and 4.4 m.		
	Thermocouple type T from Omega	Temperature in the water tank	1
	Air temperature and relative humidity sensor from Extech	Weather conditions during the test	1

the energy piles. A benchmark (6 m deep) was installed near the slab to account for slab settlements.

To avoid a power disconnection, a 3-kW Honda portable power generator was used as the power source for the instruments and tools at the site. A central hole hydraulic jack of 500 kN capacity was used to apply the load on the nail. The circulated water in the pipes was stored in a small tank. The water was circulated from the tank to the energy pile using a ½ HP portable cast iron water pump at a flow rate of 1.08 L/s.

5 Instrumentation

The energy pile was instrumented to monitor the main tests variables: displacement, strains, temperature, and relative humidity. Table 1 summarizes the instruments used.

The central steel bar was instrumented with six strain gages at different level to track the strains that developed in the pile under thermo-mechanical loading. The strain gauges used for the test were model UFCA-5-11 from Tokyo Sokki Kenkyujo Co. Ltd. Full Wheatstone bridge strain gauges with temperature and bending compensation were used. At the same level as the strain gauges, six thermocouples type T from OMEGA were installed in both the pile and adjacent borehole. The thermocouples in the pile tracked the temperature changes at the center of the energy pile in order to relate the changes in strain with the changes in temperature. The thermocouples in the adjacent borehole tracked the temperature in the soil due to the thermal use of the pile. A load cell model 3000 from GEOKON was used to measure the applied load at the pile. In addition, and for a double check, the load on the pile was measured from the pressure gauges installed on the hydraulic jack. Dial gauges were placed at the top of the energy pile to measure the vertical pile displacement. Part of the instruments were connected to read out boxes and data loggers in order to electronically store the measured data, and the other part was read manually. The air temperature and relative humidity during the test were recorded using a temperature and relative humidity USB data logger from Extech.

6 In situ test plan

Five tension load tests were performed on the energy pile referred to as Test 1, Test 2, Test 3, Test 4, and Test 5 with a tension force T of 40, 100, 150, 200, and 256 kN, respectively, applied at the top of the pile. In each test, the pile was mechanically loaded for 1 h (60 min). After 1 h of applying the load, the water pump was turned on to circulate the water into the pile. The water was heated by the high temperature weather and the work done by the water pump, resulting in an increase in circulating water temperature of 10–15 °C. The water pump was run for 4 h after finishing the mechanical loading step. The total time of the test was 5 h (300 min). During this time, the pile and soil temperature, axial strain in the pile, air temperature and relative humidity, and circulating water temperature was monitored using the instrumentation described in the previous section. The full-scale test sequence is visualized in Fig. 5 with the time on the horizontal axis and the applied tension load on the vertical axis. The shaded area under each test represents the time frame when thermal load was applied.

The loading setup showing the hydraulic jack and pump, water pump, power generator, water tank, readout boxes and data logger, and load cell is shown in Fig. 6. The pile load tests were performed from August 2 to 6, 2013, starting with Test 1 and ending with Test 5. Each day, one load step was applied; by the end of the test, the pile was unloaded and the water pump was turned off. Prior to the beginning of the testing, the strain gauge readings were

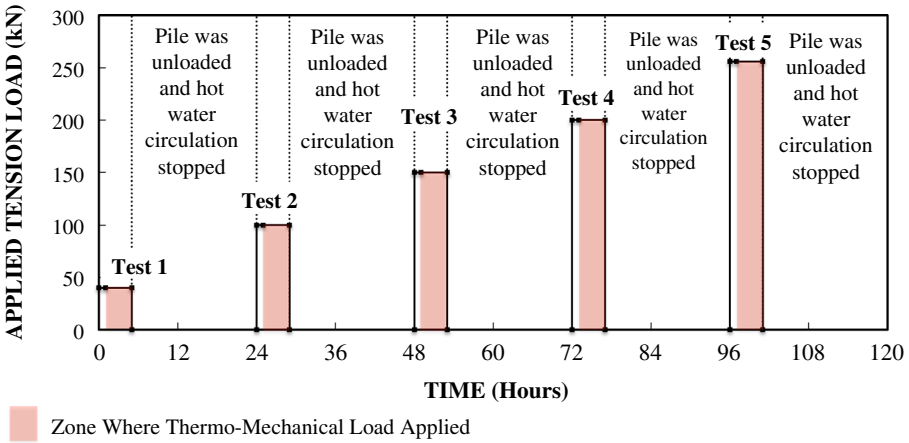

Fig. 5 Full-scale test schedule

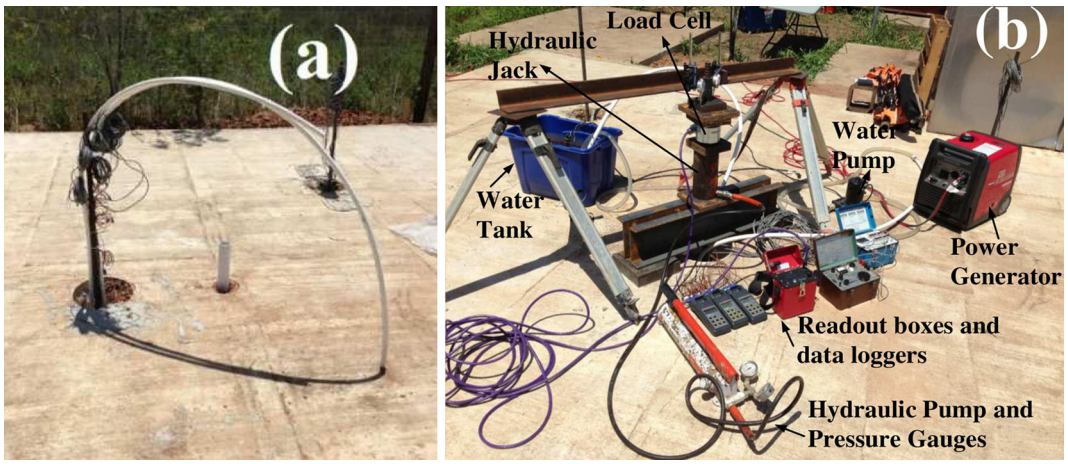

Fig. 6 **a** Tested pile, **b** test setup

zeroed, and therefore, any strains resulting from the construction process was neglected and only strains due to mechanical and thermal load were measured. The test reported in this paper was performed on pile N7 (Fig. 4).

7 Test results

In this section, the main results obtained during the tests are presented for the different stages considered in the field experiments. First the variation of temperature in the pile and soil is presented alongside of the air temperature and relative humidity fluctuations during the tests. Then the movements of the pile during the loading tests are introduced. Finally, the distribution of loads along the pile during the tests is presented.

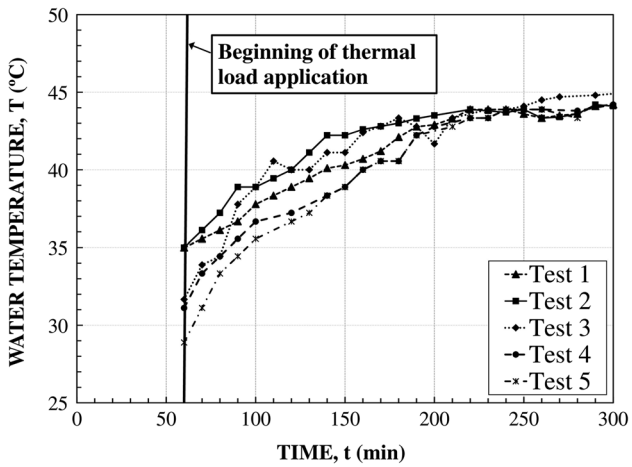

Fig. 7 Circulating water temperature during each test

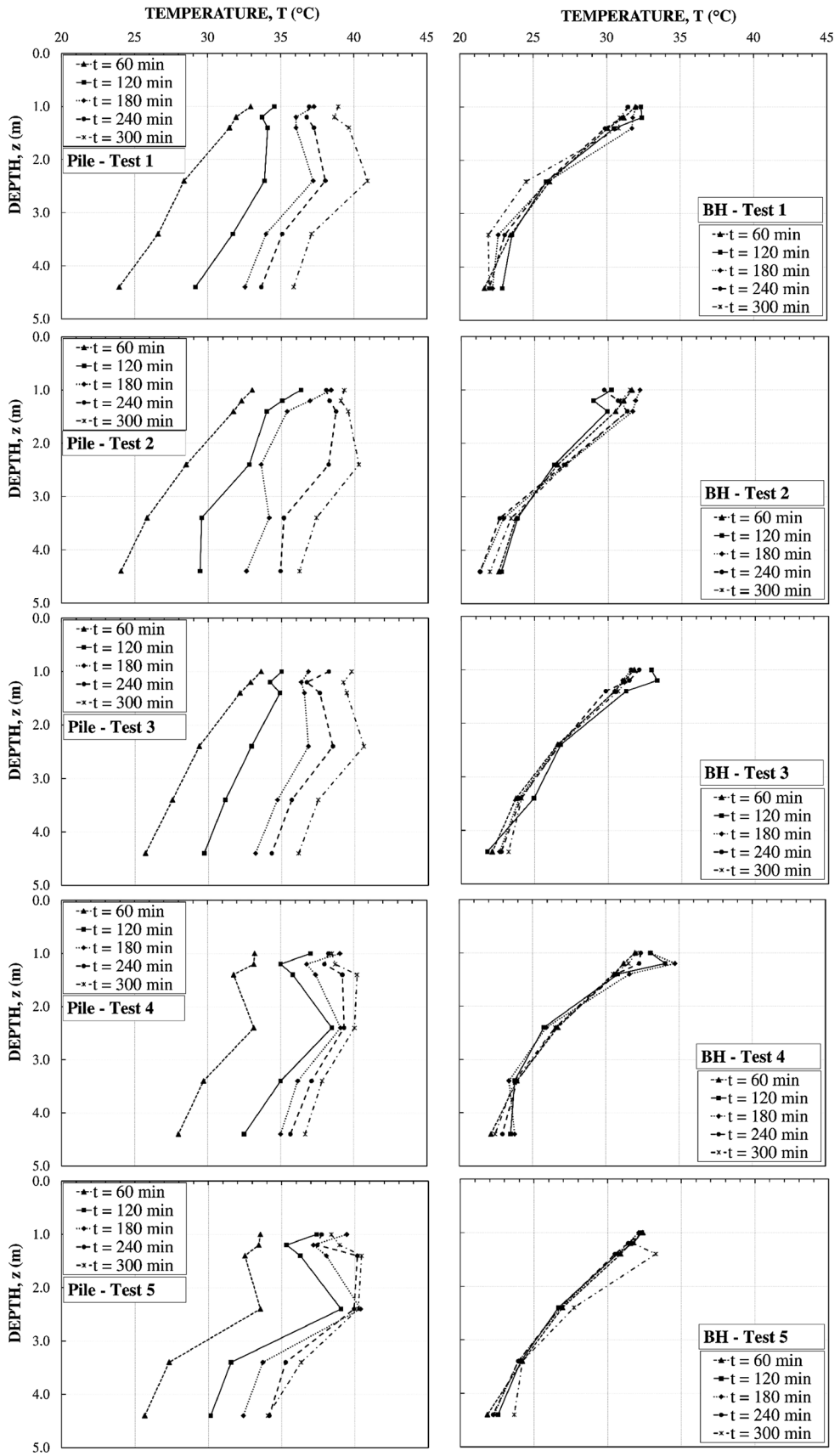

Fig. 8 **a** Pile and **b** soil temperature during the test at different times and load steps

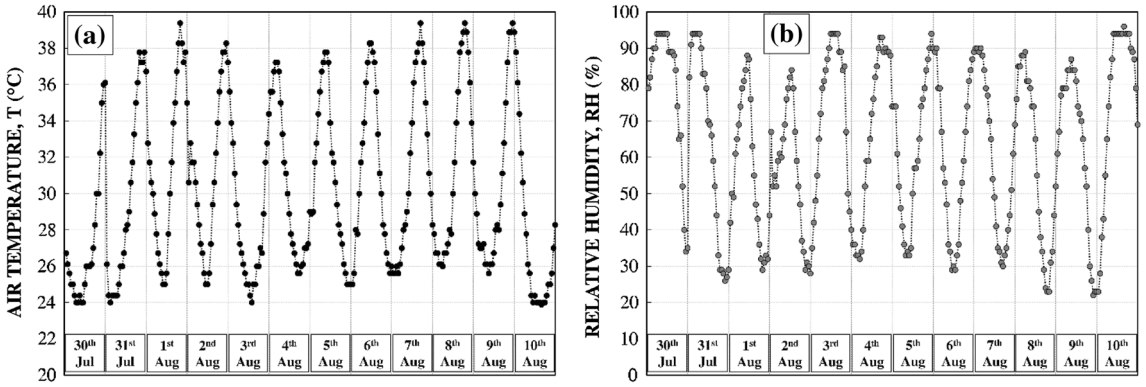

Fig. 9 **a** Air temperature and **b** air relative humidity

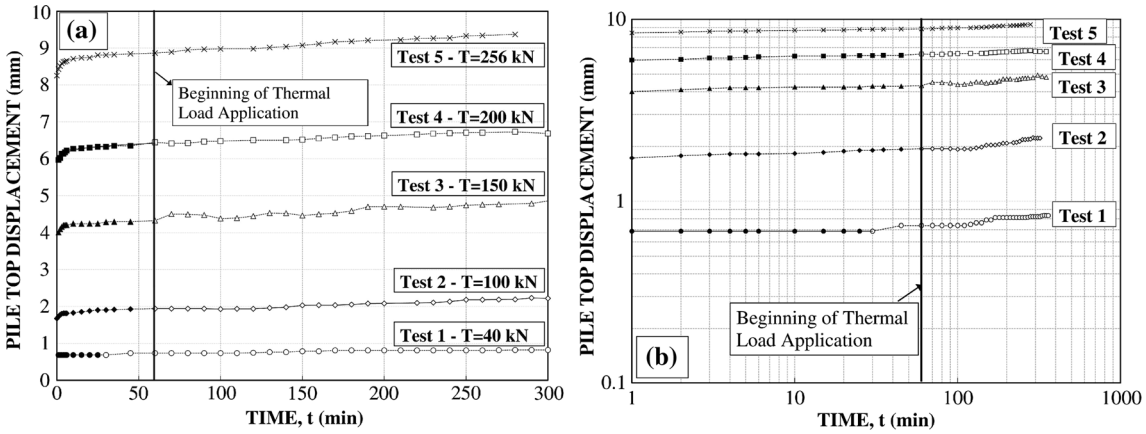

Fig. 10 **a** Pile head displacement on a natural; **b** log–log scale

7.1 Pile, soil, water, and air temperature

During each test, the pile, soil, circulating water, and ambient-air temperature were monitored using the instrumentation described in the previous section. The circulating water temperature (Fig. 7) increased during the five tests to an average value of 44 °C.

During the five tests, the temperature gradient between the circulating water and the soil generated a heat flux from the pipes toward the concrete and the soil resulting in an increase in the pile and soil temperature. The initial soil and pile temperatures were not uniform, since the pile was located in the shallow soil layer where the soil temperature is variable and highly affected by climatic conditions. As a result, the temperature gradient between the circulating water and soil was not uniform, which caused a non-uniform increase in pile temperature. Figure 8 shows the pile and soil (BH) temperature for the five tests at time $t = 60$, 120, 180, 240, and 300 min where time $t = 60$ min corresponds to the beginning of thermal load application and $t = 300$ min corresponds to the end of the test. The position BH corresponds to borehole 1 (Fig. 4, identified as BH1). The overall average pile temperature by the end of the test was 38.5 °C. There was a very small fluctuation in soil temperature at the borehole location that can be due to instruments and thermocouples; however, this fluctuation can be neglected and the average temperature profile in BH1 can be used as a reference temperature to the temperature in the pile during the test. The air temperature and relative humidity during the period when the test was performed were recorded and are presented in Fig. 9. Air temperature ranged from 24 to 39 °C with an average of 30 °C while the relative humidity ranged from 22 to 96 % with an average of 63 %.

8 Pile head load movement

The load–settlement behavior of foundation piles directly impacts on the serviceability and safety of the structure above it. To determine the amount of pile displacement associated with cyclic thermal loading of energy piles, dial

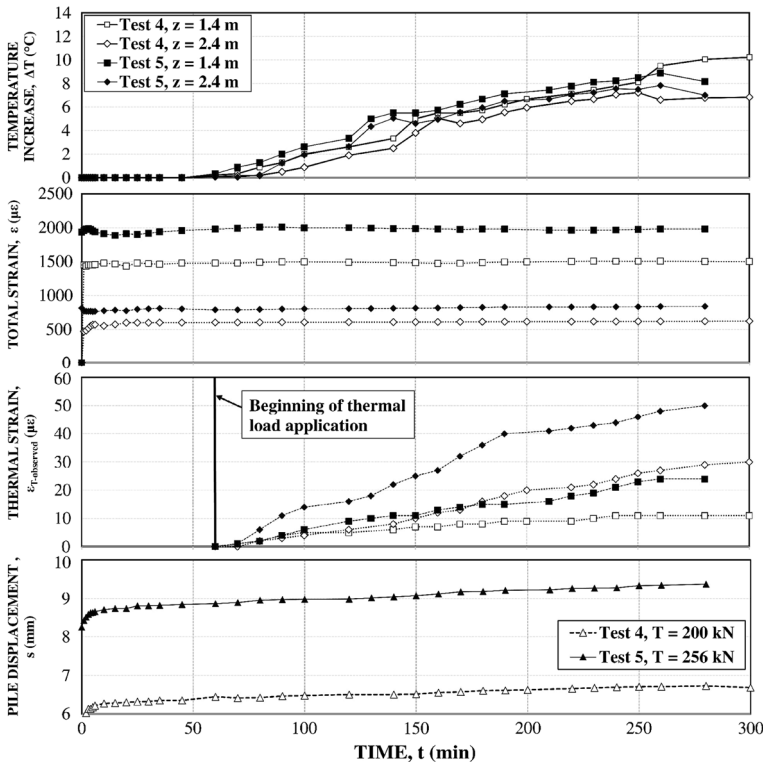

Fig. 11 Measured temperature, strain, and pile top displacement

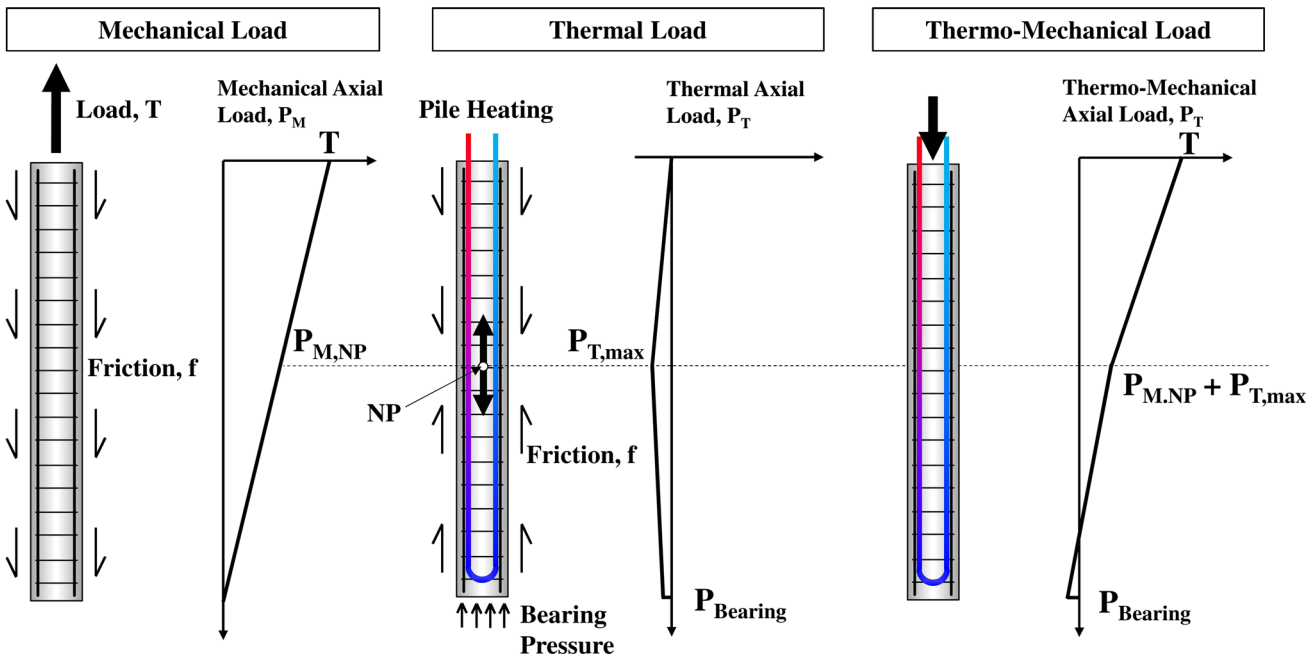

Fig. 12 Load distribution in energy piles due to mechanical, thermal, and thermo-mechanical load

gages were used during each of the five load steps (Fig. 6). The load on the pile was kept constant during each test, and the displacement versus time was measured. Figure 10a shows the pile displacement on a natural scale, while Fig. 10b shows the pile displacement on a log–log scale for creep analysis. At the application of the tension load ($t = 0$ min), the pile exhibited a rapid increase in displacements for the first few minutes. This increase then

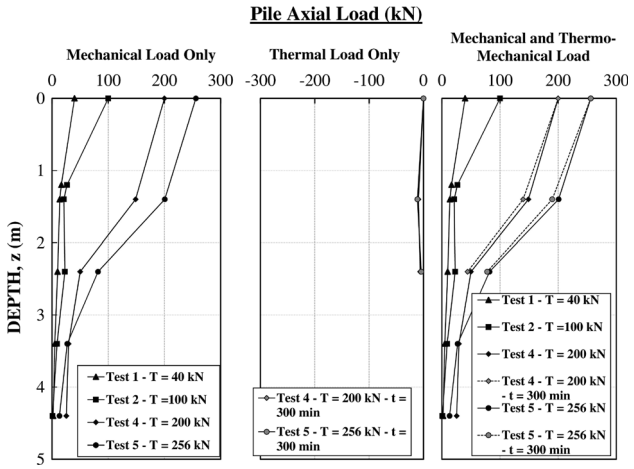

Fig. 13 Measured load distribution in the pile

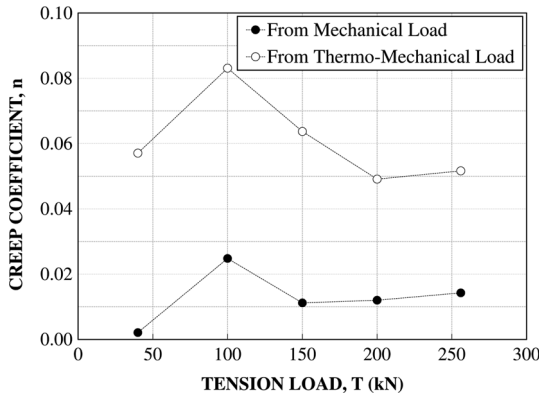

Fig. 14 Creep exponent (n) versus tension load

slowed with time and became a nearly constant rate before applying the thermal load. After applying the thermal load ($t = 60$ min), the displacement rate began to increase with the increasing temperature of the pile and the soil.

8.1 Strain gauge reading and load distribution in the pile

The strain and temperature distribution changes during the test were monitored at different positions to learn about the pile deformation and the load distribution in the pile. The most relevant data of strain distribution is presented in Fig. 11. These data correspond to the temperature, total strain, and thermal strain change in the pile at depths of 1.4 and 2.4 m during Tests 4 and 5, where the applied tension was 200 and 256 kN, respectively. In addition, the associated pile top displacement for these tests is presented on the same plot (Fig. 11).

Based on the approach proposed by Bourne-Webb et al. [13], the expected load distribution in the pile due to the thermo-mechanical load is illustrated in Fig. 12. Due to the mechanical load, the load P_M decreases linearly with depth with the maximum located at the top of the pile and equal to the applied tension, T. Due to the heating process, a tension force P_T resulting from the restrained strains develops along the pile with a maximum at the NP location, $P_{T,max}$, and with a value of $P_{Bearing}$ at the bottom of the pile. The thermo-mechanical load in the pile is the sum of the mechanical and thermal load. Negative sign represents compression load, while positive sign represents tension load.

The load distribution (Fig. 13) along the pile was calculated according to the method described in Sect. 2 (Conceptual Background) starting with the application of the load at $t = 0$ min (Mechanical load only). On the same Figure, the load distribution during Test 4 and 5 at depths 1.4 and 2.4 m resulting from the thermal load is plotted. The sum of the mechanical and thermal load is presented on the same figure (thermo-mechanical load). The concrete tensile strain capacity is 150 με or less [1]. Since the strains in the concrete were all larger than 150 με (Fig. 11), it is possible that the concrete was cracked and the steel bar took all the force in the pile element. An inspection of Fig. 13 indicates that the measured load distribution conforms to the approach described conceptually in Fig. 12.

The central reinforcing rebar yielded before reaching the ultimate tension capacity of the pile; therefore, the ultimate pile–soil friction f_u (kPa) could not be determined from the in situ test. However, data from previous static pile load test [3, 25] at the site location were used to determine f_u. Kubena and Briaud [25] back-calculated f_u, and the results ranged from 113 to 143 kPa with an average of 132 kPa in the first layer where the energy pile is embedded. Ballouz et al. [3] measured an overall average f_u along 9.5 m long, 0.92 m diameter pile of 110 kPa, but the load distribution in the pile shows a f_u of 164 kPa in the first layer. Based on these measurements, the ultimate tension capacity of the tested energy pile was calculated as 460 kN.

9 Analysis and discussion

The measurements show that the load distribution in piles is affected when the pile is used as a ground heat exchanger for SGES. It is known that the friction angle is practically independent of temperature (e.g., [16]). The thermal expansion of the pile due to an increase in temperature resulted in a change in pile–soil friction. This change in the friction profile causes a change in the load distribution; thermally induced tension load is generated in the pile. However, this change is insignificant when comparing the

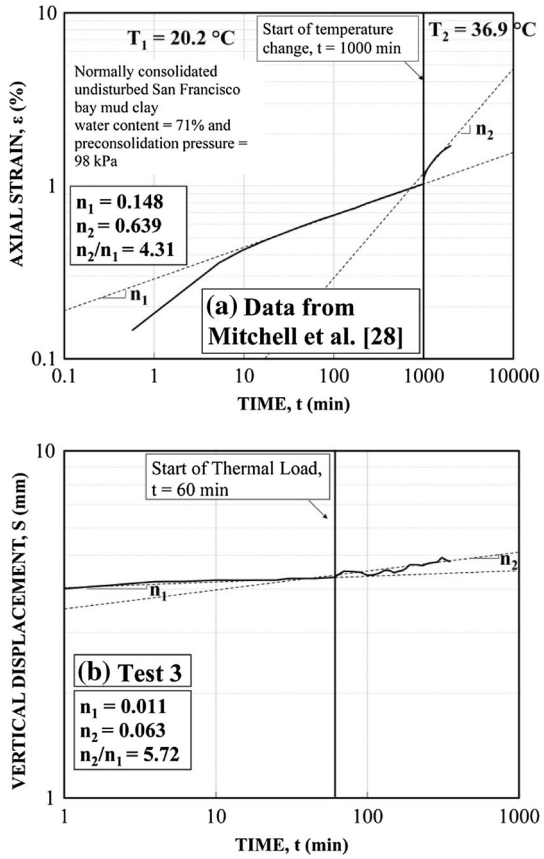

Fig. 15 Comparison of creep exponents to data from the literature

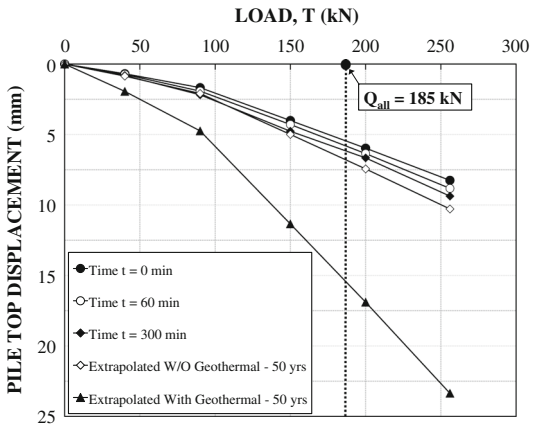

Fig. 16 Measured and extrapolated load–settlement curve

measured change in pile load to the ultimate tension capacity.

The viscous exponent n (2) was evaluated for the five tests from the displacement–time curve on the log–log scale before and after applying the thermal load (Fig. 10). The measured data were used to back calculate n using Eq. 2 together with the data from $t = 0$ to 60 min for the mechanical load only, and from $t = 60$ to 300 min for the thermo-mechanical load. The average exponent values for the mechanical and thermo-mechanical loading were 0.013 and 0.061, respectively (Fig. 14). It was therefore found that in this case when the soil is subjected to thermal loading (in addition to mechanical loading), the creep exponent increases on the average by a factor of 4.7.

The measured results from the load tests were compared to the results reported by Mitchell et al. [30] in terms of viscous exponent ratio of thermo-mechanical load (n_2) to the mechanical load (n_1), n_2/n_1. This was done by plotting the strain versus time measurement from Fig. 1 in a log–log scale and compared it with the displacement–time results from Test 3 (Fig. 15). The viscous exponents of the two tests are different by a ratio of 10 which is not surprising as the clay tested by Mitchell et al. [30] is much softer than the clay tested in this study, but the ratio n_2/n_1 of the two tests is close. Note that the ratio of the viscous exponents in Fig. 15b is for Test 3.

The long-term performance of energy piles in terms of displacement (i.e., instantaneous plus creep) was evaluated based on the measurements of the viscous exponent from the in situ test. This analysis was done by extrapolating the load–settlement curve measured at time $t = 0$ min using (2) and the measured viscous exponent. The extrapolation was performed for a structure life time of 50 years without and with geothermal use of energy piles by using 'n' from the mechanical load and from the thermo-mechanical load results, respectively. Figure 16 presents the measured load–settlement curve at the time of load application ($t = 0$ min), at 60 min, and at the end of the thermo-mechanical load ($t = 300$ min). The extrapolated load–settlement curves are plotted on the same graph in Fig. 16. The extrapolation shows that long-term displacement increases by a factor of approximately 2.35 due to creep when piles are used for geothermal energy application. However, this calculation was done assuming that the soil–pile will be subjected to heating during its life time. In reality, especially in cooling-dominated climates, the pile-heating process will only take place for 6–8 months of the year. During the rest of the year, the pile will be under cooling or idle mode. Therefore, the creep rate will slow down due to the decrease in soil temperature, and the values predicted in this paper correspond to an extreme case. The actual values should be between the extrapolated curves with and without geothermal piles. It is also worth mentioning that this analysis considers the effect of the friction (i.e., vertical/side) resistance only.

10 Conclusion

A thermo-mechanical tension load test on an energy pile in high plasticity stiff clays was presented. The strain and

temperature distribution, load–displacement behavior, and climatic conditions were monitored during the test. Based on the soil type, soil profile, soil properties, and the testing conditions, the following conclusion could be made:

1. The use of foundation piles for geothermal energy application induces thermal strains and stresses in the pile element due the volume expansion/contraction of the pile and the soil–pile friction generated from this thermally induced volume change. However, the thermally induced pile load is practically insignificant (<1 % per °C of temperature increase) compared to the ultimate values.
2. The increase in soil temperature caused an increase in the creep rate. Mathematically, this is translated by an increase in the viscous exponent n by a factor of 4.7. The measured results were compared to data from the literature and showed good consistency.
3. The time-dependent behavior of energy piles in high plasticity clays for cooling-dominated climates is an important factor to consider. The increase in the soil viscous component results in an increase in long-term displacement.
4. The distribution of energy piles should be as symmetric as possible under structures to avoid differential settlement and distortion resulting from the thermally induced deformation of the piles.
5. The extrapolated load–displacement curve of an energy piles under the tested conditions for the extreme case considered (i.e., Building cooling mode only) shows that the long-term displacement (50 years) for the energy pile is 2.35 times the displacement for the regular pile.
6. The design of energy piles in conditions similar to the ones presented in this paper should minimize the long-term displacement to tolerable limits by minimizing the initial settlement.
7. Further investigation on the time-dependent behavior of energy piles should be made through more load tests considering different soil types and in both heating and cooling conditions.

Acknowledgments This work was supported by the Buchanan Chair at Texas A&M University. The authors also appreciate the advice and support of Dave Weatherby with Schnabel Foundation.

References

1. ACI Committee 224. ACI Report 224R-01, Control of cracking in concrete structures
2. Amatya B, Soga K, Bourne-Webb P, Amis T, Laloui L (2012) Thermo-mechanical behaviour of energy piles. Géotechnique 62 6:503–519
3. Ballouz M, Nasr G, Briaud JL (1991) Dynamic and static testing of nine drilled shafts at Texas A&M University geotechnical research sites research Report to FHWA, Civil Engineering. Texas A&M University, Texas
4. Blum P, Campillo G, Munch W, Kolbel T (2010) CO_2 savings of ground source heat pump systems—A regional analysis. Renew Energy 35(2010):122–127
5. Brandl H (1998) Energy piles and diaphragm walls for heat transfer from and into the ground. Proc 3rd Int Symp. On deep foundations on bored and auger piles, BAP III, Ghent, 37–60
6. Brandl H (2006) Energy foundations and other thermo-active ground structures. Géotechnique 56 No. 2: 81–122, http://dx.doi.org/10.1680/geot.2006.56.2.81
7. Briaud JL (1993) National geotechnical experimentation sites at Texas A&M University: clay and sand data collected until 1992. Report No. NGES-TAMU-001, Department of Civil Engineering, Texas A&M University, College Station, Texas
8. Briaud JL (1997) The national geotechnical experimentation sites at Texas A&M University: clay and sand. report No. NGES-TAMU-007, Department of Civil Engineering, Texas A&M University, College Station, Texas
9. Briaud JL, Powers WF, Weatherby DE (1998) Should grouted anchors should have short tendon bond length. J Geotech Geoenvironmental Eng 124(2), ASCE, New York
10. Briaud JL (2013) The pressuremeter test: expanding its use. The 2013 Louis Menard lecture, Proceeding of the 18th international conference on soil mechanics and geotechnical engineering. ENPC Press, Paris
11. Briaud J-L (2013) Geotechnical engineering: unsaturated and saturated soils. Wiley, New York, pp 1000
12. Bruner RF, Marcontell M, Briaud JL, National geotechnical experimentation sites at Texas A&M University: Clay and Sand. Survey of the sites, 1993 (1994) Report No NGES-TAMU-002, Department of Civil Engineering. Texas A&M University, College Station
13. Bourne-Webb P, Amatya B, Soga K, Amis T, Davidson C, Payne P (2009) Energy pile test at Lambeth College, London: geotechnical and thermodynamic aspects of pile response to heat cycles. Géotechnique 59 3:237–248
14. Burghignoli A, Desideri A, Miliziano S (2000) A laboratory study on the thermomechanical behaviour of clayey soils. Can Geotech J 37 4:764–780
15. Campanella RG, Mitchell JK (1967) Temperature effects on volume changes and pore pressures in soils. J SMFD, ASCE 94(3)
16. Cui YJ, Le TT, Tang A, Delage P, Li X (2009) Investigating the time-dependent behaviour of Boom clay under thermo-mechanical loading. Géotechnique 59 4:319–329
17. Cekerevac C, Laloui L (2004) Experimental study of thermal effects on the mechanical behavior of a clay. Int J Numer Anal Methods in Geomech, 28 no. 3(0): pp 209–228
18. De Bruyn D, Thimus JF (1996) The influence of temperature on mechanical characteristics of Boom clay: the results of an initial laboratory program. Eng Geo 41, No. 1–4, 117
19. Environmental Protection Agency (EPA) (1993) Space conditioning: the next frontier. The potential of advanced residential space conditioning technologies for reducing pollution and saving money. EPA 430-R-93-004
20. Farouki OT (1986). Thermal properties of soils. Series on rock and soil mechanics. Vol. 11. Trans Tech Publ, Clausthal-Zellerfeld, Germany
21. Hueckel T, Pellegrini R (1992) Effective stress and water pressure in saturated clays during heating–cooling cycles. Can Geotech J 29:1095–1102
22. International Ground Source Heat Pump Association (2009) Ground source heat pump residential and light commercial design and installation guide. Oklahoma State University

23. Jennings SP, Mathewson CC, Yancey TE, Briaud JL (1986) National geotechnical experimentation sites at Texas A&M University: clay and sand, geology Report No. NGES-TAMU-005, Department of Civil Engineering, Texas A&M University, College Station, Texas
24. Kalantidou A, Tang AM, Pereira JM, Hassen G (2012) Preliminary study on the mechanical behaviour of heat exchanger pile in physical model. Géotechnique 62, No.11, 1047–1051. http://dx.doi.org/10.1680/geot.11.T.013)
25. Kubena ME, Briaud JL (1989) Capacity of 2 drilled and grouted piles. research Report 5887-2F to minerals management service, Civil Engineering, Texas A&M University, 1989
26. Laloui L, Moreini M, Vulliet L (2003) Comportement d'un pieu bi-fonction, fondation et échangeur de chaleur. Can Geotech J 40 2:388–402
27. Laloui L, Nuth M, Vulliet L (2006) Experimental and numerical investigation of the behavior of a heat exchanger pile. Int J Numer Anal Methods Geomech 30 8:763–781
28. McCartney JS, Rosenberg JE (2011) Impact of heat exchange on the axial capacity of thermo-active foundations. Proceedings Geo-Frontiers 2011 (GSP 211). In: Han J, Alzamora DE (eds) ASCE, Reston VA. pp 488–498
29. Mitchell JL, Campanella RG (1964). Creep studies on saturated clays. Symposium on laboratory shear testing of soils, ASTM-NRC, Ottawa, Canada, ASTM Special Tech. Publication no. 361, September 1963
30. Mitchell JK, Campanella RG, Singh A (1968) Soil creep as a rate process. J SMFD, ASCE 94(1)
31. McCartney JS, Murphy KD (2012) Strain distributions in full-scale energy foundations. DFI J 6(2):28–36
32. Marcontell M, Briaud JL (1994) National geotechnical experimentation sites at Texas A&M University: clay and sand data collected from January 1993 to July 1994, Report No NGES-TAMU-003, Department of Civil Engineering, Texas A&M University, College Station, Texas
33. McCormac CJ, Brown HR (2009) Design of reinforced concrete. Wiley, New York
34. Olgun GC, Martin JR, Abdelaziz SL, Iovino PL, Catalbas F, Elks C, Fox C, Gouvin P (2012) Field testing of energy piles at Virginia Tech. Proceedings of the 37th annual conference on deep foundations, 2012, Houston, TX, USA
35. Romero E (1999) Characterization and thermal-hydro-mechanical behaviour of unsaturated Boom clay: an experimental study. PhD Thesis, Technical University of Catalonia, Spain
36. Simon P, Briaud JL (1996) National geotechnical experimentation sites at Texas A&M University: Clay and Sand, Soil Data in Electronic Form, 1995–1996, Report No. NGES-TAMU-006, Department of Civil Engineering, Texas A&M University, College Station, Texas
37. Sultan N, Delage P, Cui YJ (2002) Temperature effects on the volume change behaviour of Boom clay. Eng Geol 64(2–3):135–145
38. Tao C, Briaud JL (1995) National experimentation sites at Texas A&M University: clay and sand, soil data in electronic form, 1977–1955, Report No. NGES-TAMU-004, Department of Civil Engineering, Texas A&M University, College Station, Texas